Crystal structure and Biological evolution of 5-bromothiophene based 3,4-dihydropyrimidin-2-(1H)-thi(ones)

Venkatachalam Ramkumar
Indian Institute of Technology Madras
Ramesh Gardas
Indian Institute of Technology Madras
Sourav Banerjee
University of Dundee
Hitendra Patel (hm_patel@spuvvn.edu)
Sardar Patel University
Mayank Sharma
Sardar Patel University
Ruturajsinh Vala
Sardar Patel University
Dhanji Rajani
Micro care Laboratory

Research Article

Keywords: DHPMs, Antibacterial activity, Antifungal activity, Hirshfeld surfaces Analysis, ADMET prediction

Posted Date: July 19th, 2021

DOI: https://doi.org/10.21203/rs.3.rs-721141/v1

Abstract

Herein, Solvent-free synthesis of 5-bromothiophene based 3,4-dihydropyrimidin-2-(1*H*)-thi(ones) was explored. The main advantages of this study are that pure product comes in hand with easy workup and without using any separation technique, a good amount of yield, and formation of product in crude form. We developed a single crystal of **4c**, and we analysed crystal structure by Hirshfeld surfaces analysis. All the synthesised compounds were screened for antifungal and antibacterial assay. Among all synthesised compounds, **4a**, **4b** and **4j** have potent antibacterial activity. While **4f**, **4g**, **4h** and **4i** show good antifungal activity among all synthesised compounds. We also carried out ADMET prediction for the **4(a-j)**, and calculated data show that all the compounds have prominent drug-like nature.

1. Introduction

Dihydropyrimidine-thi(ones) (DHPMs) are prominent compounds exhibiting a wide range of pharmacological properties such as antiproliferative,[1] antiviral,[2] antioxidant,[3,4] anti-carcinogenic,[5] anti-HIV[6], antimicrobial and antitubercular activities.[7] Medicinal chemistry efforts have led to the development of various DHPMs based lead compounds. For example, monastrol is well known inhibitor of the mitotic kinesin Eg5,[8] (R)-mon-97 is a potent antimitotic inhibitor,[9] (R)-SQ 32926 reported as antihypertensive agent[10] and MAL1-271 increases the ATPase activity of a eukaryotic Hsp70.[11]

On a similar note, 5-bromothiophene bearing compounds have many applications and have successfully been used to form metal complexes[12,13] and specific polymers.[14] Interestingly, Pd(0)-catalysed Suzuki–Miyaura cross-coupling reactions led to the development of biologically potent 5-bromothiophene molecules.[15,16] Hence, both DHPM and 5-bromothiophene exhibit exciting biological potency individually. In our previous work, we synthesised 5-bromothiophene based 1,4-dihydropyridine [17] and Mannich products [18] with good antibacterial and antifungal activities. Therefore, development of 5-bromothiophene based 3,4-dihydropyrimidin-2-(1H)-thi(ones) could prove as worthy pharmacological tools.

For this purpose, we decided to utilise the Biginelli reaction to develop 5-bromothiophene based 3,4-dihydropyrimidin-2-(1H)-thi(ones). Like many other reactions, [19–25] Biginelli reaction is a three-component reaction involving the condensation of an aldehyde, urea and a β-ketoester under acidic conditions.[26] In our previous work, we synthesised 5-bromothiophene based 1,4-dihydropyridine via solvent-free protocol for CAN (Ceric ammonium nitrate) catalysed Hantzsch reaction.[17] In the current study, we utilised the same protocol for the Biginelli reaction and successfully produced 5-bromothiophene based DHPMs with potent biological activity. We further screened the novel 5-bromothiophene based DHPMs for antibacterial and antifungal activity and established the in silico ADME prediction which shows promising drug-likeness for the synthesised molecules.

2. Result And Discussion

2.1. Chemistry

To optimise the reaction condition, we carried out trial reactions with 5-bromothiophene-2-carboxaldehyde (**1**, 1mmol), ethyl acetoacetate (**2c**, 1mmol), and urea (**3a**, 1mmol) using CAN as a catalyst in different reaction conditions (Table 1).

In optimisation of reaction, our first target is to carry out the reaction at ambient temperature, but with this reaction we got lower yields at ambient temperature (Entry 2 and 3, Table 1). So, we carried out the reactions at 60°C with different amounts of catalyst at different reaction times, in which we got the best result with 20 mol % of CAN at 70 minutes (Entry 6, Table 1). The reaction was also optimised with different solvents, but we got the sticky product on work up except DMF, which is tedious to handle, while we got the crude product in solvent-free condition.

After these experiments, we further go with the solvent-free reaction. The targeted compounds **4(a-j)** were synthesized from 5-bromothiophene-2-carboxaldehyde (**1**, 1mmol), ketoester (**2a-2e**, 1mmol), and urea/thiourea (**3a-3b**, 1mmol) using CAN (20

mol %) as catalyst in solvent-free condition at 60°C with average reaction time of 60–90 minutes (Table 2).

We successfully carried out the solvent-free synthesis of compounds **4(a-j)** using CAN as a catalyst within 60–90 minutes of heating at 60°C. Structures of the synthesised compound were confirmed by spectral analysis, for which spectral data are given in supplementary material.

In ^{1}H-NMR spectra, signals at δ 0.8–1.5 ppm confirm the presence of methyl group at C-1, whereas, for methyl, ethyl, iso-butyl, tert-butyl of ester give signals in a range of δ 1.5–3.0 ppm. A signal that appears as a singlet at a range of δ 5.0–6.0 ppm confirms the presence of proton at γ-position. For aromatic protons, we observe signals in the range of δ 6.8–7.6 ppm. For 2 –NH groups in some of the compounds, we observe singlet for both after an aromatic region in between δ 8.0-9.5 ppm and in some cases, we got singlet for 1 –NH around δ 6.0 ppm and for another around δ 8.5 ppm.

In ^{13}C-APT spectra, signals in a range of δ 16–18 ppm confirm the presence of a methyl group, whereas signal for other aliphatic carbons of the ester group appears in the range of δ 30–55 ppm. For the quaternary carbon of the ring, we observe signals in a range of δ 100–110 ppm and signals in a range of δ 160–170 ppm that confirms the presence of the carbonyl group. Single-crystal XRD analysis of **4c** also confirmed its structure.

2.2. Molecular structure of 4c

2.2.1. Description of crystal structure

The single-crystal structural data indicate that **4c** was crystallised in P1 space group. The molecule of **4c** is not symmetrical (Fig. 1a). The asymmetric unit revealed two molecules of **4c**, and one of them contains a distorted thiophene ring. Pyrimidinone ring in **4c** is observed in half chair configuration. Triclinic unit cell of crystal with cell dimensions a = 7.3244(3) Å, b = 13.5742(6) Å, c = 14.8486(7) Å, α = 94.044(2)°, β = 103.959(2)°, γ = 99.511(2)° show in Fig. 1b. In the crystal lattice, molecules of **4c** have connected via strong N-H ····O = C hydrogen bonding interactions in a zigzag fashion and overall, a layered structure is formed (Fig. 1b). Each carbonyl oxygen able to interact with two neighbour atom's hydrogens simultaneously with H ····O ····H bond angle 116.78° and 118.51°. Thus, each molecule interacts with two neighbour molecules by four hydrogen-bonding interactions having bond lengths 2.070 Å, 2.153 Å, 2.158 Å and 2.159 Å. XRD data were deposited online to Cambridge Crystallographic Data Centre (CCDC). CCDC deposition number 1970503 contains the Supporting Information crystallographic data for this paper.

2.2.2. Hirshfeld surfaces analysis

Hirshfeld surfaces for **4c** were calculated as per established procedures. [27] These calculation help to understand effect of weak intermolecular interactions into the molecular packing. In Fig. 1c Hirshfeld surfaces mapped over d_{norm} in the − 0.5530 to + 1.3583 arbitrary unit range. Broad and bright-red spots on pyrimidone ring surface and near hydrogen atom of amino groups and oxygen atom of carbonyl group respectively recognise donor and acceptor of potential N-H...O hydrogen bond. Whereas the presence of diminutive and faint-red spots on the surface characterises weak intermolecular interactions in **4c**. On thiophene ring surface, short interatomic Br···S/S···Br contacts in crystal packing of **4c** are viewed as the faint-red spots. Diminutive-red spots are also observed which indicated short interatomic H···H contacts.

The two-dimensional fingerprint plot for **4c** and fingerprint plots delineated into H··· H, O··· H/H··· O, C··· H/H··· C, Br··· H/H··· Br, S··· H/H··· S, N··· H/H··· N and Br··· S/S··· Br contacts are illustrated in Fig. 2(a-h) respectively. The H... H contacts show as a symmetrically dispersed point that covers a wide area of the plot and occupies a significant portion of the Hirshfeld area (37.5 percent) The contribution of O...H/H...O, which corresponds to the NH...O interactions, is shown by a pair of sharp dots typical of hydrogen bonds. Here, the proportions of O ... H and H ... O interactions are remarkably not identical (O ... H (8.2%) and H ... O (7.3%)). Among these three contacts, only O-H interactions, with a total de + di smaller than the sum of the Van der Waals radii of participating atoms (H: 1.09 A, O: 1.52 A), are considered close together. The remaining contacts, like N...O/O...N, O...O, C...O/O...C, and N...H/H...N, barely contribute 6.1 % to the HS. These interactions fall under the category of

far contacts in which summation di + de is higher than the sum of the van der Waals radii of the atoms, together with the C...H/H...C and H...H and contacts.

2.3. Biological evaluation

2.3.1. Antibacterial assay

The antibacterial activity of compounds **4(a-j)** was performed on gram-positive and gram-negative bacteria by broth dilution method. The screening results were summarised in Table 3. The MIC values of compounds **4(a-j)** are between 50–500 μg/mL against tested microorganisms. In the case of gram-negative bacteria, **4h** shows good antibacterial activity against E.coli than the standard drug ampicillin, while **4b** show good antibacterial activity against P.aeruginosa than standard drug ampicillin. In the case of gram-positive bacteria, **4a**, **4b**, **4d**, **4g** and **4i** show good antibacterial activity against S.aureus than standard drug ampicillin, while **4a** show good antibacterial activity against S.pyogenus. Overall, **4a**, **4b** and **4h exhibited maximal** antibacterial activity.

2.3.2. Antifungal assay

Fungicidal activities of **4(a-j)** were evaluated against three fungi C.albicans, A.niger, and A.clavatus and the minimum inhibitory concentrations were derived. The screening results were summarised in Table 4. Tabulated data show that compounds **4f**, **4g**, **4h** and **4i** are more effective on C.albicans than the standard drug griseofulvin. Entire antifungal data indicate that dihydropyrimidinthione **4(f-j)** are more potent than dihydropyrimidinones **4(a-e)**.

2.4. ADMET prediction

ADMET properties of the compound are important for its drug-like profile. It might be important for novel drug discovery.[28] Physicochemical properties of the compounds correlate to their drug-likeness via various rules like Lipinski's, Ghose's, Veber's Egan's and Muegee's rule. Physicochemical properties must stay within limits defined in each rule. We evaluate our synthesised compounds for their ADMET properties with the help of the online web server SwissADME. (http://www.swissadme.ch) Calculated physicochemical properties of **4(a-j)** are summarised in Table 5. The value of physicochemical properties remains in the limits defined for Lipinski's, Ghose's, Veber's, Egan's, and Muegee's rule. Thus, all 5-bromothiophene based DHPMs incorporate all rule of drug-likeness, so they have good drug-like potential. Bioavailability radar of the compounds were derived based on six physicochemical properties namely lipophilicity, size, polarity, solubility, flexibility and saturation. The bioavailability radar showed that all **4(a-j)** molecules exhibited drug-like radar plots (Bioavailability radar graph of **4(a-j)** were included in supporting information file**).**

To predict the gastrointestinal absorption and blood-brain barrier permeability of the compounds, BOILED-Egg delineation was used. BOILED-Egg delineation of all the synthesised compounds is illustrated in Fig. 3. The white, elliptical region of the egg depicts a high probability of gastrointestinal absorption, while the yellow (Yolk) region of the egg depicts blood-brain permeation of molecule.[29] All 5-bromothiophene based DHPMs show high gastrointestinal absorbance, and they have no blood-brain permeability. Red dots for all the **4(a-j)** denoted that they are not P-gp substrate.

3. Conclusion

In summary, we successfully carried out the synthesis of compounds **4(a-j)** in solvent-free condition using CAN as an efficient catalyst with easy workup procedure, eco-friendly synthetic route and without the use of any hazardous solvent or any separation technique. Antibacterial data show that our synthesised 5-bromothiophene based DHPMs have good antimicrobial activity. Furthermore, it also showed that dihydropyrimidinthione **4(f-j)** have more potent antifungal activity compared to dihydropyrimidinones **4(a-e).** *In silico* ADME prediction confirmed that 5-bromothiophene based DHPMs have a good drug-like profile.

4. Methods And Materials

4.1. General

All chemicals were purchased from commercially available sources and were used without further purification. The progress of the reaction was monitored by silica gel 60 F254 (Merck) coated TLC plates. Reported R_f values correspond to elution with 1:4 (n-hexane: ethyl acetate) mobile phase. Melting points were determined by the open capillary tube method and are uncorrected. IR spectra were recorded on an ABB MB3000 spectrophotometer. ^{1}H NMR and ^{13}C-APT spectral analyses were recorded using a BRUKER AVANCE II 400 NMR spectrometer. Abbreviations used for the ^{1}H-NMR signal are as follows: s = singlet, d = doublet, t = triplet, dd = double doublet, q = quartet, m = multiplet. The chemical shifts are expressed in parts per million. coupling constants (*J*) are provided in Hertz.

4.2. General procedure for synthesis of compounds 4(a-j).

5-bromothiophene-2-carboxaldehyde **1** (1 mmol), ketoester **2(a-f)** (1 mmol), and urea / thiourea **3(a-b)** (1 mmol) and CAN (20 mol %) as catalyst were taken into 50 ml round bottom flask. Then the reaction mixture was stirred at 60°C for 60–90 minutes. After completion of this reaction time (single spot were observed on TLC) which indicates the formation of product. After that the crude was extracted with 2 ml of ethyl acetate and then poured in 8 ml of n-hexane, where the crude yellow/brown product was formed. The product was filtered and further recrystallized with ethanol.

4.2.1. 5-acetyl-4-(5-bromothiophen-2-yl)-6-methyl-3,4-dihydropyrimidin-2(1 H)-one (4a): ^{1}H-NMR: ($CDCl_3$, 400 MHz), δ = 2.09(3H, s), 2.32 (3H, s), 5.45 (1H, s), 6.64 (1H, *J* = 5.2 Hz, d), 6.85 (1H, *J* = 5.2 Hz, d), 8.03 (1H, s), 8.43 (1H, s) ppm; ^{13}C-APT: ($CDCl_3$, 100 MHz), δ = 18.7, 26.3, 51.1, 110.1, 127.5, 129.0, 138.0, 144.2, 148.1, 152.1, 165.4 ppm; IR: 3321, 3315, 3011, 2959, 1744, 1656, 1593, 1054, 1467, 1373, 1329, 1244, 1123, 585 cm^{-1}; Anal. Calcd for $C_{11}H_{11}BrN_2O_2S$: C, 41.92; H, 3.52; N, 8.89; Found: C, 41.87; H, 3.49; N, 8.81.

4.2.2. Methyl-4-(5-bromothiophen-2-yl)-6-methyl-2-oxo-1,2,3,4-tetrahydropyrimidine-5-carboxylate (4b): ^{1}H-NMR: ($CDCl_3$, 400 MHz), δ = 2.37(3H, s), 3.76(3H, s), 5.61(1H, s), 6.74(1H, *J* = 3.6 Hz, d), 6.88(1H, *J* = 3.6 Hz, d), 8.03(1H, s), 8.43(1H, s) ppm; ^{13}C-APT: ($CDCl_3$, 100 MHz), δ = 18.3, 34.8, 51.3, 102.5, 112.6, 125.1, 129.6, 144.0, 146.8, 165.3, 167.5, 175.2 ppm; IR: 3437, 3318, 3080, 3130, 2895, 1744, 1656, 1587, 1486, 1392, 1154, 1123, 1035, 576 cm^{-1}; Anal. Calcd for $C_{11}H_{11}BrN_2O_3S$: C, 39.89; H, 3.35; N, 8.46; Found: C, 39.82; H, 3.29; N, 8.42.

4.2.3. ethyl-4-(5-bromothiophen-2-yl)-6-methyl-2-oxo-1,2,3,4-tetrahydropyrimidine-5-carboxylate (4c): ^{1}H-NMR: (DMSO-d_6, 400 MHz), δ = 1.17(3H, *J* = 7.2 Hz, t), 2.23(3H, s), 4.06(2H, *J* = 7.2 Hz, q), 5.35(1H, s), 6.73(1H, *J* = 3.2 Hz, d), 7.05(1H, *J* = 3.6 Hz, d), 7.49(1H, s), 9.37(1H, s) ppm; ^{13}C-APT: (DMSO-d_6, 100 MHz),14.6, 18.2, 50.0, 60.0, 99.6, 110.2, 124.8, 130.4, 149.7, 150.9, 152.6, 165.4 ppm; IR: 3469, 3419, 3005, 3098, 2967, 2905, 1769, 1650, 1512, 1478, 1389, 1336, 1265, 1119, 1034, 583 cm^{-1}; Anal. Calcd for $C_{12}H_{13}BrN_2O_3S$: C, 41.75; H, 3,80; N, 8.11; Found: C, 41.68; H, 3.73; N, 8.02.

4.2.4. isobutyl-4-(5-bromothiophen-2-yl)-6-methyl-2-oxo-1,2,3,4-tetrahydropyrimidine-5-carboxylate (4d): ^{1}H-NMR: (DMSO-d_6, 400 MHz), δ = 0.83(6H, *J* = 4.8 Hz, d), 1.16(1H, m), 2.25(3H, s), 3.62(2H, *J* = 6.4 Hz, q), 5.34(1H, s), 6.73(1H, *J* = 4.8 Hz, d), 7.05(1H, *J* = 6.0 Hz, d), 7.95(1H, s), 9.43(1H, s) ppm; ^{13}C-APT: ($CDCl_3$, 100 MHz), δ = 13.6, 19.0, 27.7, 48.7, 70.3, 101.3, 123.4, 130.3, 133.3, 141.3, 147.0, 153.0, 165.4 ppm; IR: 3408, 3355, 3002, 3083, 2995, 2954, 1751, 1648, 1597, 1499, 1343, 1370, 1025, 1120, 1255, 538 cm^{-1}; Anal. Calcd for $C_{14}H_{17}BrN_2O_3S$: C, 45.05; H, 4.59; N, 7.50; Found: C, 44.92; H, 5.51; N, 7.52.

4.2.5. tert-butyl-4-(5-bromothiophen-2-yl)-6-methyl-2-oxo-1,2,3,4-tetrahydropyrimidine-5-carboxylate (4e): ^{1}H-NMR: ($CDCl_3$, 400 MHz), δ = 1.33(9H, s), 2.26(3H, s), 5.65(1H, s), 6.77(1H, *J* = 2.8 Hz, d), 7.07(1H, *J* = 4.0 Hz, d), 8.44(1H, s), 9.35(1H, s) ppm; ^{13}C-APT: ($CDCl_3$, 100 MHz), δ = 13.6, 18.3, 28.2, 49.00, 80.4, 102.3, 123.2, 130.2, 133.0, 141.6, 145.9, 153.4, 164.7 ppm; IR: 3483, 3419, 3193, 3061, 2928, 2940, 1735, 1662, 1587, 1524, 1471, 1386, 1342, 1123, 1161, 1035, 545 cm^{-1}; Anal. Calcd for $C_{14}H_{17}BrN_2O_3S$: C, 45.05; H, 4.59; N, 7.50; Found: C, 44.98; H, 4.56; N, 7.43.

4.2.6. 1-(4-(5-bromothiophen-2-yl)-6-methyl-2-thioxo-1,2,3,4-tetrahydropyrimidin-5-yl)ethanone (4f): ^{1}H-NMR: (CD_3OD, 400 MHz), δ = 2.03(3H, s), 2.34(3H, s), 5.53(1H, s), 6.76(1H, *J* = 3.6 Hz, d), 6.93(1H, *J* = 3.6 Hz, d) ppm; ^{13}C-APT: (CD_3OD, 100 MHz), δ = 16.7, 34.6, 50.1, 100.2, 110.61, 122.8, 124.0, 129.0, 129.4, 148.7, 149.8, 153.6, 166.0 ppm; IR: 3489, 3442, 3061,

2996, 2950, 1735, 1642, 1586, 1029, 1122, 1254, 1484, 1379, 1336, 568 cm^{-1}; Anal. Calcd for $C_{11}H_{11}BrN_2OS_2$: C, 39.88; H, 3.35; N, 8.46; Found: C, 39.79; H, 3.31; N, 8.38.

4.2.7. Methyl-4-(5-bromothiophen-2-yl)-6-methyl-2-thioxo-1,2,3,4-tetrahydropyrimidine-5-carboxylate (4g): ^{1}H-NMR: ($CDCl_3$, 400 MHz), δ = 2.34(3H, s), 3.75(3H, s), 5.60(1H, s), 6.44(1H, S), 6.73(1H, S), 6.82(1H, s), 8.49(1H, s) ppm; ^{13}C-APT: ($CDCl_3$, 100 MHz), δ = 18.7, 19.5, 34.8, 51.5, 101.0, 111.8, 123.3, 124.2, 129.3, 129.5, 147.4, 148.5, 153.7, 165.6 ppm; IR: 3470, 3415, 3067, 2978, 1751, 1660, 1596, 1066, 1243, 1119, 1475, 1373, 576 cm^{-1}; Anal. Calcd for $C_{11}H_{11}BrN_2O_2S_2$: C, 38.05; H, 3.19; N, 8.07; Found: C, 38.00; H, 3.12; N, 7.99.

4.2.8. ethyl-4-(5-bromothiophen-2-yl)-6-methyl-2-thioxo-1,2,3,4-tetrahydropyrimidine-5-carboxylate (4h): ^{1}H-NMR: ($CDCl_3$, 400 MHz), δ = 1.27(3H, *J* = 7.2 Hz, t), 2.33(3H, s), 4.18(2H, *J* = 7.2 Hz, q), 5.61(1H, s), 6.50(1H, s), 6.73(1H, *J* = 3.2Hz, d), 6.88(1H, s), 8.46(1H, s) ppm; ^{13}C-APT: ($CDCl_3$, 100 MHz), δ = 14.3, 18.6, 50.8, 60.4, 101.3, 111.8, 124.2, 129.5, 147.1, 148.7, 153.8, 165.2ppm; IR: 3428, 3418, 3055, 2962, 1743, 1636, 1599, 1034, 1173, 1234, 1497, 583 cm^{-1}; Anal. Calcd for $C_{12}H_{13}BrN_2O_2S_2$: C, 39.89; H, 3.63; N, 7.75; Found: C, 39.81; H, 3.54; N, 7.71.

4.2.9. isobutyl-4-(5-bromothiophen-2-yl)-6-methyl-2-thioxo-1,2,3,4-tetrahydropyrimidine-5-carboxylate (4i): ^{1}H-NMR: ($CDCl_3$, 400 MHz), δ = 0.90(6H, s), 2.28(1H, m), 2.40(3H, s), 3.79(4H, m), 5.72(1H, s), 5.91(1H, s), 6.77(1H, s), 7.07(1H, s), 8.24(1H, s) ppm; IR: 3425, 3312, 3055, 2962, 1744, 1636, 1497, 1034, 1173, 1234, 1497, 1505, 1392, 682 cm^{-1}; Anal. Calcd for $C_{14}H_{17}BrN_2O_2S_2$: C, 43.19; H, 4.40; N, 7.20; Found: C, 43.13; H, 4.36; N, 7.16.

4.2.10. tert-butyl-4-(5-bromothiophen-2-yl)-6-methyl-2-thioxo-1,2,3,4-tetrahydropyrimidine-5-carboxylate (4j): ^{1}H-NMR: (CD_3OD, 400 MHz), δ = 1.16(9H, s), 1.96(3H, s), 4.48(1H, s), 6.68(1H, *J* = 4.8 Hz, d), 6.85(1H, *J* = 5.2 Hz, d), 7.85(1H, s), 8.16(1H, s) ppm; IR: 3444, 3312, 3084, 2950, 2895, 1743, 1657, 1589, 1485, 1033, 1144, 1234, 1336, 1386, 583 cm^{-1}; Anal. Calcd for $C_{14}H_{17}BrN_2O_2S_2$: C, 43.19; H, 4.40; N, 7.20; Found: C, 43.09; H, 4.32; N, 7.12.

4.3. Antimicrobial assay (Antibacterial and antifungal assay)

in vitro anti-microbial activity was investigated against Gram-positive, Gram-negative bacteria and three fungi by the disc diffusion method according to the National Committee for Clinical Laboratory Standards (NCCLS). [30] The synthesized compounds 4(a-j) were screened for their antibacterial activity against Gram-negative bacteria like E.coli, P.aeruginosa, Gram-positive bacteria like S.aureus, S.pyogenus and fungal stain like C.albicans A.niger and A.clavatus. Ampicillin used as standard drugs for the comparison of antibacterial activity and griseofulvin was used as standard drugs for the antifungal activity.

Declarations

Acknowledgement

Authors are thankful to SERB, New Delhi, India for providing financial assistance from major research project (File No.EEQ/2016/000376, dated 07/02/2017). We also thankful to UGC, New Delhi for UGC-CPEPA Phase-II program sponsored under award letter no. F. No. 1–14/2002-2016(NS/PE) dated 28th April 2016 for the assistance in general and NMR facility in particular. SB is funded by Ninewells Cancer Campaign Cancer Research Award.

Author contribution

MGS was involved in the synthesis, conception and design of the study. RMV was involved in acquisition of data, analysis and interpretation of data and *in silico* study. DPR was involved in *in vitro* antibacterial and antifungal activity. VR and RLG were involved in single-crystal XRD study. SB and HMP were involved in drafting and revising of the manuscript.

Conflicts of interests

The authors declare that there are no conflicts of interests.

References

1. Vala, R. M. *et al.* Synthesis and in vitro study of antiproliferative benzyloxy dihydropyrimidinones. *Arch. Pharm*, **354**, 2000466 https://doi.org/10.1002/ardp.202000466 (2021).
2. Kumarasamy, D. *et al.* Synthesis and in vitro antiviral evaluation of 4-substituted 3,4-dihydropyrimidinones. *Bioorganic & medicinal chemistry letters*, **27**, 139–142 https://doi.org/10.1016/j.bmcl.2016.12.010 (2017).
3. Padmavathy, K. *et al.* Synthesis, Antioxidant Evaluation, Density Functional Theory Study of Dihydropyrimidine Festooned Phenothiazines. **3**,5965–5974, doi: https://doi.org/10.1002/slct.201800748 (2018).
4. Padmavathy, K. *et al.* Synthesis, Antioxidant Evaluation, Density Functional Theory Study of Dihydropyrimidine Festooned Phenothiazines. *ChemistrySelect* **3**, 5965–5974, doi:https://doi.org/10.1002/slct.201800748 (2018).
5. de Souza, V. P. *et al.* Hybrid 3,4-dihydropyrimidin-2-(thi)ones as dual-functional bioactive molecules: fluorescent probes and cytotoxic agents to cancer cells. *New Journal of Chemistry*, **44**, 12440–12451 https://doi.org/10.1039/D0NJ01368D (2020).
6. Kim, J. *et al.* A novel 3,4-dihydropyrimidin-2(1H)-one: HIV-1 replication inhibitors with improved metabolic stability. *Bioorganic & medicinal chemistry letters*, **22**, 2522–2526 https://doi.org/10.1016/j.bmcl.2012.01.133 (2012).
7. Patel, N., Pathan, S. & Soni, H. I. 3,4-Dihydropyrimidin-2(1H)-One Analogues: Microwave irradiated Synthesis with Antimicrobial and Antituberculosis Study. *Current Microwave Chemistry*, **6**, 61–70 https://doi.org/10.2174/2213335606666190724093305 (2019).
8. Kapoor, T. M., Mayer, T. U., Coughlin, M. L. & Mitchison, T. J. Probing spindle assembly mechanisms with monastrol, a small molecule inhibitor of the mitotic kinesin, Eg5. *J. Cell Biol*, **150**, 975–988 (2000).
9. Garcia-Saez, I. *et al.* Structure of human Eg5 in complex with a new monastrol-based inhibitor bound in the R configuration. *J. Biol. Chem*, **282**, 9740–9747 (2007).
10. Schnell, B. *et al.* Synthesis of enantiomerically pure 4-aryl-3,4-dihydropyrimidin-2(1H)-ones via enzymatic resolution: preparation of the antihypertensive agent (R)-SQ 32926†Synthesis and reactions of Biginelli compounds, part 20; for part 19, see: ; ; ; 2000, 56, 1859–1862.†. *Tetrahedron: Asymmetry* **11**, 1449–1453, doi:https://doi.org/10.1016/S0957-4166(00)00081-1 (2000).
11. Chiang, A. N. *et al.* Synthesis and evaluation of esterified Hsp70 agonists in cellular models of protein aggregation and folding. *Biorg. Med. Chem*, **27**, 79–91 https://doi.org/10.1016/j.bmc.2018.11.011 (2019).
12. Singh, K., Puri, P., Kumar, Y., Sharma, C. & Syntheses Spectral, and Biological Studies of New Imines Derived From 5-Bromothiophene-2-Carboxaldehyde and Their Si(IV), Sn(IV) Complexes. *Phosphorus, Sulfur, and Silicon and the Related Elements* **188**, 1462–1473, doi: https://doi.org/10.1080/10426507.2012.757609 (2013).
13. López, R., Villagra, D., Ferraudi, G., Moya, S. A. & Guerrero, J. Preparation and photophysical properties of precursors of inorganic macromolecules. Mono and binuclear complexes of Ru(II) and terpyridine derivatized with thiophene and 4'-(5-bromothiophene) groups. *Inorg. Chim. Acta*, **357**, 3525–3531 https://doi.org/10.1016/j.ica.2004.02.038 (2004).
14. Trumbo, D. L. & Marvel, C. S. Polymerization using palladium (II) salts II: Polymerization of 2-ethynyl-5-bromothiophene. *J. Polym. Sci., Part A: Polym. Chem*, **24**, 2231–2238 https://doi.org/10.1002/pola.1986.080240917 (1986).
15. Noreen, M. *et al.* A facile synthesis of new 5-aryl-thiophenes bearing sulfonamide moiety via Pd(0)-catalyzed Suzuki–Miyaura cross coupling reactions and 5-bromothiophene-2-acetamide: As potent urease inhibitor, antibacterial agent and hemolytically active compounds. *Journal of Saudi Chemical Society*, **21**, S403–S414 https://doi.org/10.1016/j.jscs.2014.04.007 (2017).
16. Rasool, N. *et al.* Design, synthesis, and spasmolytic activity of thiophene-based derivatives via Suzuki cross-coupling reaction of 5-bromothiophene-2-carboxylic acid: their structural and computational studies. *Turkish Journal of Chemistry*, **44**, 1410–1422 https://doi.org/10.3906/kim-1911-51 (2020).
17. Sharma, M., Rajani, D. & Patel, H. Green approach for synthesis of bioactive Hantzsch 1, 4-dihydropyridine derivatives based on thiophene moiety via multicomponent reaction. *Royal Soc. Open Sci*, **4**, 170006 (2017).

18. Patel, H., Rajani, D., Sharma, M., Bhatt, H. & Synthesis Molecular Docking and Biological Evaluation of Mannich Products Based on Thiophene Nucleus using Ionic Liquid. *Letters in Drug Design & Discovery*, **16**, 119–126 (2019).
19. Patel, D. M., Vala, R. M., Sharma, M. G., Rajani, D. P. & Patel, H. M. A Practical Green Visit to the Functionalized [1, 2, 4] Triazolo [5, 1-b] quinazolin-8 (4H) one Scaffolds Using the Group-Assisted Purification (GAP) Chemistry and Their Pharmacological Testing. ChemistrySelect 4, 1031–1041(2019).
20. Sharma, M. G., Vala, R. M. & Patel, H. M. Pyridine-2-carboxylic acid as an effectual catalyst for rapid multi-component synthesis of pyrazolo[3,4-b]quinolinones. *RSC Advances*, **10**, 35499–35504 https://doi.org/10.1039/D0RA06738E (2020).
21. Patel, D. M., Patel, H. J., Padrón, J. M. & Patel, H. M. A novel substrate directed multicomponent reaction for the syntheses of tetrahydro-spiro[pyrazolo[4,3-f]quinoline]-8,5'-pyrimidines and tetrahydro-pyrazolo[4,3-f]pyrimido[4,5-b]quinolines via selective multiple C–C bond formation under metal-free conditions. *RSC Adv*, **10**, 19600–19609 https://doi.org/10.1039/D0RA02990D (2020).
22. Patel, D. M., Patel, H. M. & Trimethylglycine-Betaine H, 5 H-spiro [[1, 3] dioxolo [4, 5-g] quinoline-7, 5'-pyrimidine]-2', 4', 6'(3' H)-trione Derivatives. *ACS Sustain. Chem. Eng*, **7**, 18667–18676 (2019). -Based-Catalyst-Promoted Novel and Ecocompatible Pseudo-Four-Component Reaction for Regioselective Synthesis of Functionalized 6, 8-Dihydro-1'
23. Sharma, M. G. *et al.* One-Pot Assembly for Synthesis of 1, 4-Dihydropyridine Scaffold and Their Biological Applications. *Polycyclic Aromat. Compd*, 1–11 https://doi.org/10.1080/10406638.2019.1686401 (2019).
24. Patel, H. M. Synthesis of new mannich products bearing quinoline nucleous using reusable ionic liquid and antitubercular evaluation. *Green Sustain. Chem*, **5**, 137 (2015).
25. Vala, R. M. *et al.* Synthesis of a novel Pyrano [2, 3-c] pyrazole enabling PKBβ/AKT2 inhibitory and in vitro anti-glioma activity, doi: https://doi.org/10.26434/chemrxiv.14774835.v1 (ChemRxiv, 2021).
26. Ranu, B. C., Hajra, A. & Jana, U. Indium (III) chloride-catalyzed one-pot synthesis of dihydropyrimidinones by a three-component coupling of 1, 3-dicarbonyl compounds, aldehydes, and urea: an improved procedure for the Biginelli reaction. *The Journal of organic chemistry*, **65**, 6270–6272 (2000).
27. Tan, S. L., Jotani, M. M. & Tiekink, E. R. T. Utilizing Hirshfeld surface calculations, non-covalent interaction (NCI) plots and the calculation of interaction energies in the analysis of molecular packing. *Acta Crystallographica Section E*, **75**, 308–318 https://doi.org/10.1107/S2056989019001129 (2019).
28. Mokariya, J. A., Kalola, A. G., Prasad, P. & Patel, M. P. Simultaneous ultrasound- and microwave-assisted one-pot 'click' synthesis of 3-formyl-indole clubbed 1,2,3-triazole derivatives and their biological evaluation. *Mol. Diversity*, https://doi.org/10.1007/s11030-021-10212-8 (2021).
29. Daina, A., Zoete, V. A. & BOILED-Egg To Predict Gastrointestinal Absorption and Brain Penetration of Small Molecules. *ChemMedChem* **11**, 1117–1121, doi:https://doi.org/10.1002/cmdc.201600182 (2016).
30. NCCLS (National Committee for Clinical Laboratory Standards) Twelfth Information Supplement, ISBN 1-56238-454-6 M100-S12 (M7), 2002.

Tables

Table1: Optimisation of reaction condition.

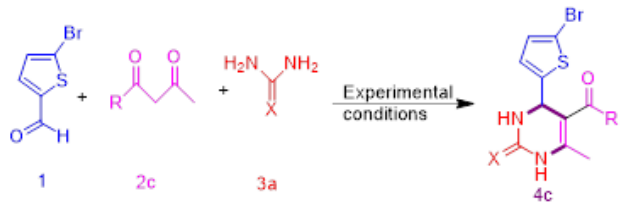

Entry	CAN (% mol)	Solvent	Condition	Time (in minutes)	Yield [b] (%)
1	--	–	60 °C	120[a]	Incomplete
2	10	–	–	30	Incomplete
3	20	–	–	30	Incomplete
4	20	–	60 °C	30 [a]	Incomplete
5	**20**	**–**	**60 °C**	**70 [a]**	**100%**
6	20	Water	60 °C	60 [a]	NIL
7	20	Ethanol	60 °C	90 [a]	100% [c]
8	20	Toluene	60 °C	90 [a]	Incomplete
9	20	Acetonitrile	60 °C	90	100% [c]
10	20	DMF	60 °C	90 [a]	100%

[a] time when stop heating; [b] isolated yield; [c] sticky product occurred

Table 2 Synthesis of compound **4(a-j)** via modified Biginelli reaction [a]

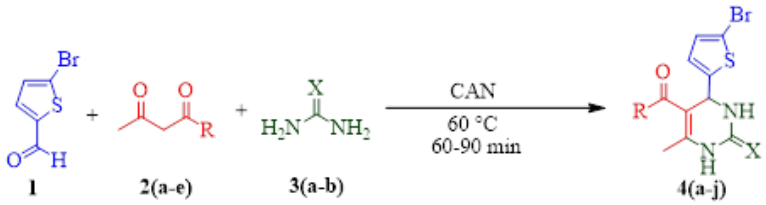

Entry	Compound	Substituent (R)	Substituent (X)	Melting point[b] (°C)	R_f value[c]	Yield[d] (%)
1	**4a**	Me	O	244-248	0.18	72
2	**4b**	OMe	O	232-236	0.22	80
3	**4c**	OEt	O	212-216	0.24	78
4	**4d**	Oi-Bu	O	242-246	0.20	74
5	**4e**	Ot-Bu	O	240-244	0.22	76
6	**4f**	Me	S	228-232	0.12	66
7	**4g**	OMe	S	221-223	0.14	70
8	**4h**	OEt	S	202-205	0.10	72
9	**4i**	Oi-Bu	S	236-238	0.12	68
10	**4j**	Ot-Bu	S	242-246	0.14	73

[a] reaction condition: 1 mmol 5-bromothiophene-2-carboxaldehyde **1**, 1 mmol β-keto ester **2(a-f)**, and 1 mmol urea/thiourea **3(a-b)**, 20 mol % CAN, 60 °C, 60-90 min; [b] melting points are determined by open capillary method; [c] TLC was run in n-hexane: ethyl acetate, 1:4 elution; [d] isolated yield.

Table 3: Antibacterial activity (MIC value) in µg/mL of the synthesised compounds **4(a-j)**

Entry	Compounds	*Gram-negative bacteria*		*Gram-positive bacteria*	
		E.coli	*P.aeruginosa*	*S.aureus*	*S.pyogenus*
1	**4a**	100	250	**125**	**50**
2	**4b**	125	**50**	**62.5**	250
3	**4c**	125	100	500	250
4	**4d**	125	100	**125**	250
5	**4e**	250	500	500	250
6	**4f**	125	250	250	250
7	**4g**	125	250	**100**	200
8	**4h**	**62.5**	100	250	125
9	**4i**	250	125	**125**	100
10	**4j**	250	500	250	100
11	AMPICILLIN	100	100	250	100

Table 4: Antifungal activity (MIC value) in µg/mL of the synthesised compounds **4(a-j)**

Sr. No.	Compounds	*C.ALBICANS*	*A.NIGER*	*A.CLAVATUS*
1	**4a**	500	>1000	>1000
2	**4b**	500	>1000	>1000
3	**4c**	1000	>1000	>1000
4	**4d**	500	1000	>1000
5	**4e**	500	1000	1000
6	**4f**	**250**	500	500
7	**4g**	**250**	1000	>1000
8	**4h**	**250**	500	>1000
9	**4i**	**100**	500	500
10	**4j**	500	250	250
11	GRISEOFULVIN	500	100	100

Table 5 Physicochemical properties of **4(a-j)** and various filters for drug-likeness

Comp.	MW	RB	HBA	HBD	MR	TPSA	XLOGP	WLOGP	MLOGP	NR	NC	NH	Atom
4a	315.19	2	2	2	77.46	86.44	1.58	1.64	1.42	2	11	6	28
4b	331.19	3	3	2	78.55	95.67	1.75	1.23	1.4	2	11	7	29
4c	345.21	4	3	2	83.35	95.67	2.12	1.62	1.67	2	12	7	32
4d	373.27	5	3	2	92.97	95.67	3.08	2.25	2.18	2	14	7	38
4e	373.27	4	3	2	93.01	95.67	2.74	2.39	2.18	2	14	7	38
4f	331.25	2	1	2	84.66	101.46	2.18	1.81	1.46	2	11	6	28
4g	347.25	3	2	2	85.75	110.69	2.35	1.39	1.42	2	11	7	29
4h	361.28	4	2	2	90.56	110.69	2.72	1.78	1.69	2	12	7	32
4i	389.33	5	2	2	100.17	110.69	3.68	2.42	2.2	2	14	7	38
4j	389.33	4	2	2	100.21	110.69	3.34	2.56	2.2	2	14	7	38

Abbreviation: MW: Molecular Weight; RB: Rotational Bond; HBA: H-Bond Acceptor; HBD: H-Bond Donor; MR: Molecular Refractivity; TPSA: Topological Polar Surface Area; NR: No. of ring; NC: No. of Carbon; NH: No. of Heteroatoms

Lipinski Filter	Ghose filter	Veber filter	Egan filter	Muegge filter
MW ≤ 500	160 ≤ MW ≤ 480	RB ≤ 10	WlogP ≤ 5.88	200 ≤ MW ≤ 600;
MlogP ≤ 4.15	-0.4 ≤ WlogP ≤ 5.6	TPSA ≤ 140		-2 XlogP ≤ 5; TPSA ≤ 150
HBA ≤ 10	40 ≤ MR ≤ 130		TPSA ≤ 131.6	NR ≤ 7; NC > 4; NH > 1; RB ≤ 15; HBA ≤ 10; HBD ≤ 5
HBD ≤ 5	20 ≤ atoms ≤ 70			

Figures

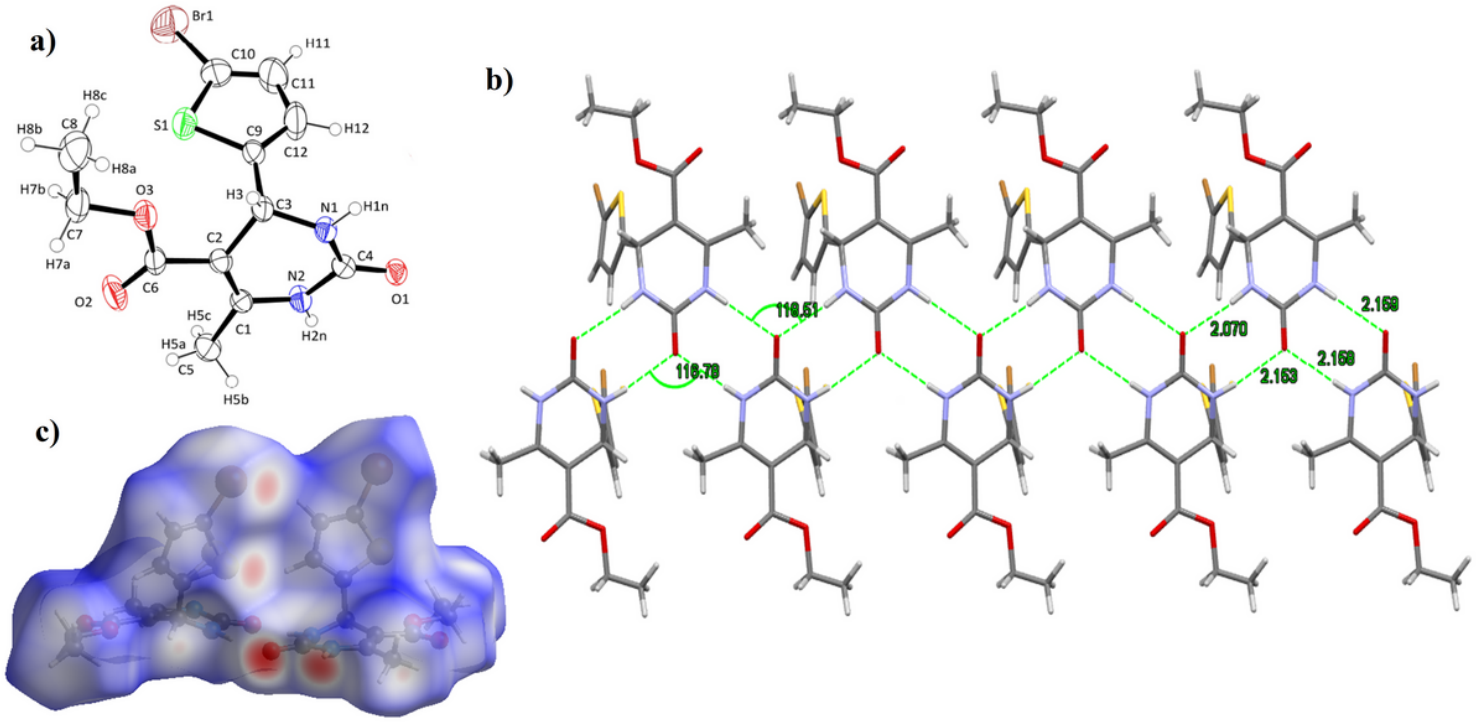

Figure 1

a) ORTEP view of the compound 4c with displacement ellipsoids drawn at 40%. H atoms are shown as small spheres of arbitrary radii. b) Packing arrangement presenting single layer with intermolecular (C=O···H-N) hydrogen bonding interaction. c) Views of Hirshfeld surface around molecule of 4c which mapped over dnorm in - 0.5530 to +1.3583 arbitrary unit range.

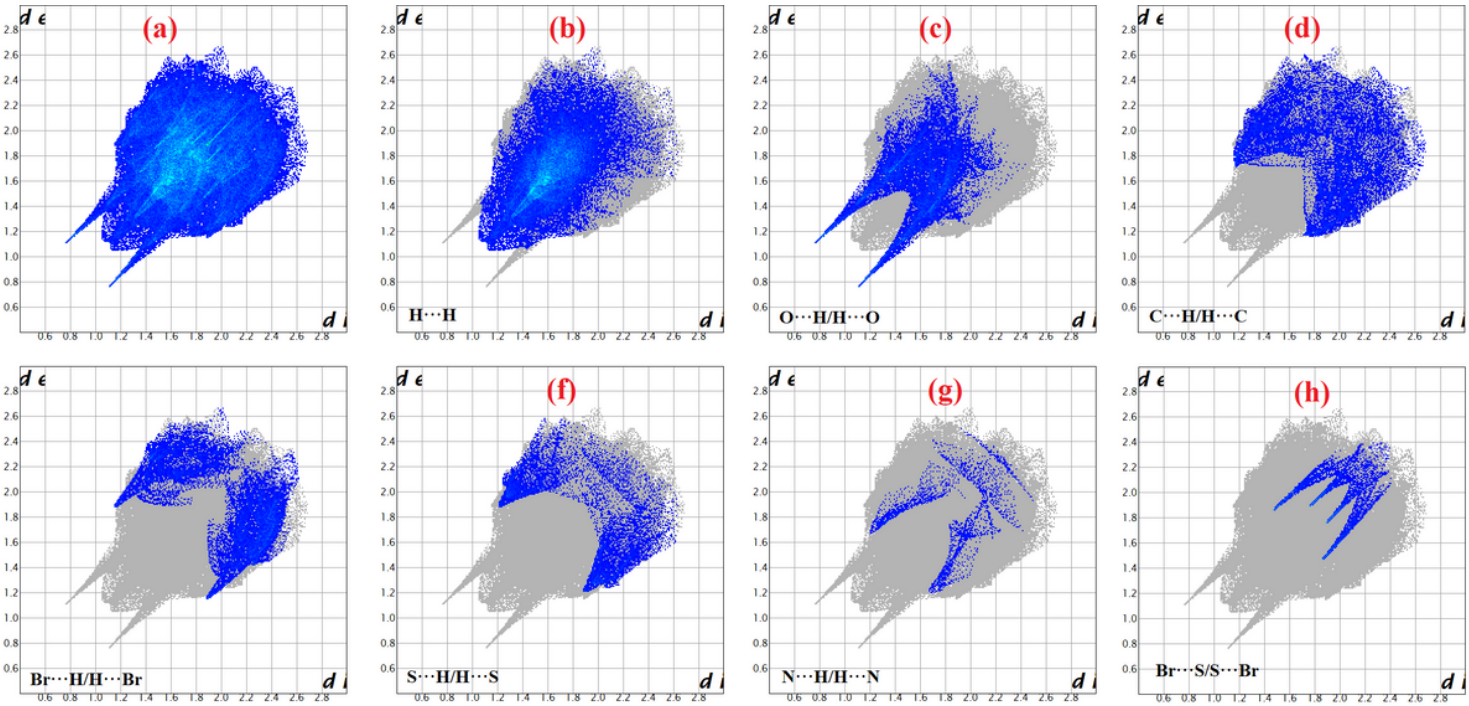

Figure 2

Two-dimensional fingerprint plot for 4c which deline into various contacts.

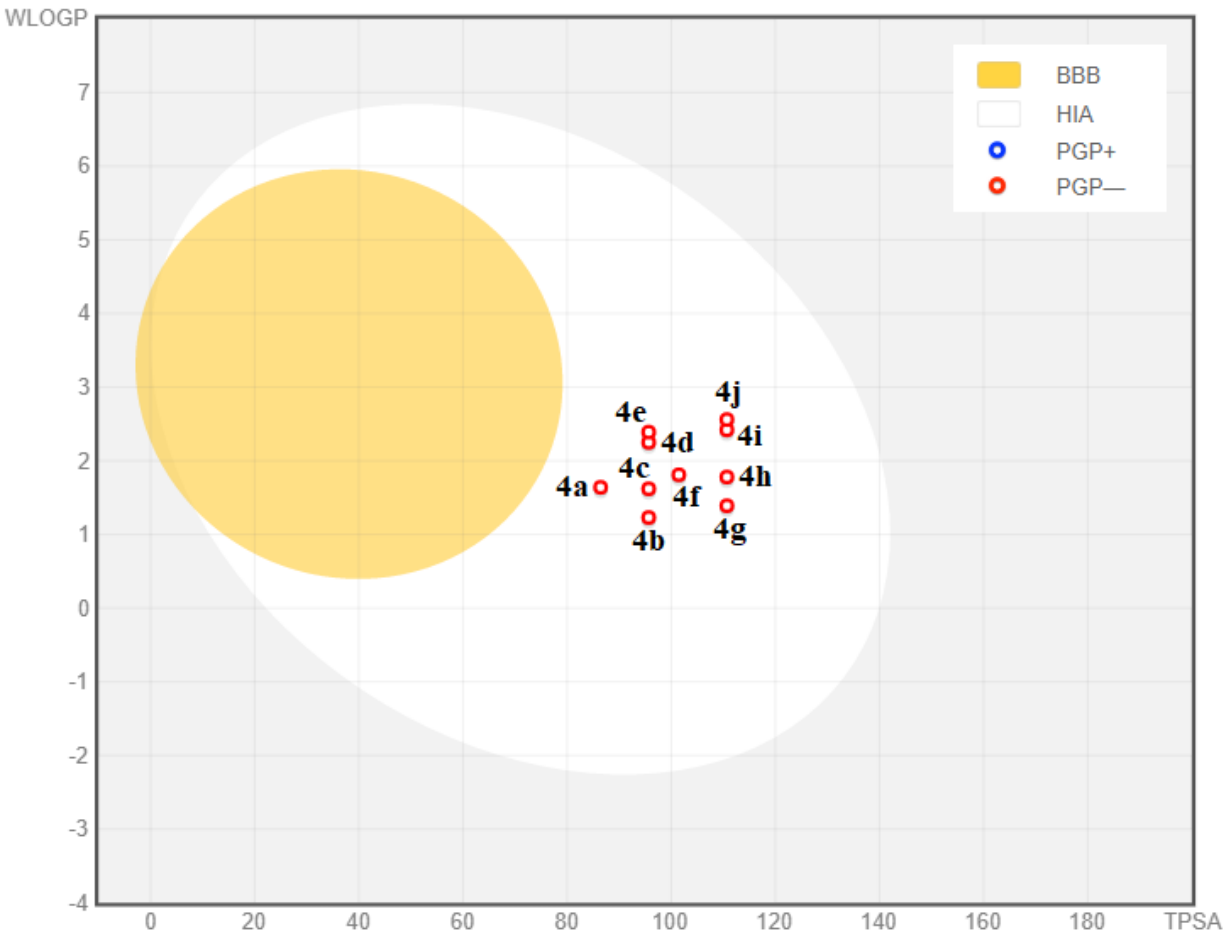

Figure 3

BOILED-Egg model of 5-bromothiophene based DHPMs 4(a-j)

Supplementary Files

This is a list of supplementary files associated with this preprint. Click to download.

- supplementaryfiles15.07.2021.docx